Supersymmetry in carbon nanotubes in a transverse magnetic field

H.-W. Lee

Department of Physics, Pohang University of Science and Technology, Pohang, Kyungbuk 790-784, Korea

Dmitry S. Novikov

Department of Physics, Center for Materials Sciences & Engineering,
Massachusetts Institute of Technology, Cambridge, Massachusetts 02139, USA

(Dated: February 6, 2008)

Electron properties of carbon nanotubes in a transverse magnetic field are studied using a model of a massless Dirac particle on a cylinder. The problem possesses supersymmetry which protects low-energy states and ensures stability of the metallic behavior in arbitrarily large fields. In metallic tubes we find suppression of the Fermi velocity at half-filling and enhancement of the density of states. In semiconducting tubes the energy gap is suppressed. These features qualitatively persist (although to a smaller degree) in the presence of electron interactions. The possibilities of experimental observation of these effects are discussed.

I. INTRODUCTION

The electronic properties of single-walled carbon nanotubes (NT) vary for tubes with different structure. Depending on the angle between the tube axis and graphite lattice, called the NT chiral angle, the tube electron spectrum can be metallic or semiconducting.[1] The semiconducting band gap of a single-walled NT (SWNT) is of the order of $1\,\mathrm{eV}$ and scales inversely with the NT radius R. Also, in many nominally metallic tubes a minigap appears at the band center due to the intrinsic tube curvature.[2–4] These gaps, recently observed experimentally,[5,6] have the size of a few tens of millivolts for SWNT's and scale as $1/R^2$ with the NT radius.

Ajiki and Ando have made a remarkable observation[7] that in nanotubes the metallic behavior is fragile: a metallic NT can be easily turned into a semiconducting one by applying a relatively weak parallel magnetic field. Such a field, by inducing backscattering between right and left electron modes, opens a minigap at the band center. This gap, linear in the field, is given by the magnetic flux scaled by the flux quantum, $\pi R^2 B/\Phi_0$, times the semiconducting gap size. For $B \simeq 10$ T the gap is of the order of $10\,\mathrm{meV}$ for typical SWNT radii. Effects of parallel field on multi-walled NT's have been reported in Ref.[8]. Electronic properties are also sensitive to mechanical distortion, such as twisting, bending, or squashing,[9–11] as well as to external electric fields.[12,13]

Another interesting observation made in Ref.[7] is that a transverse magnetic field affects electron states in a way completely opposite to the parallel field effect. In metallic tubes the Fermi velocity is suppressed by a transverse field, while the density of states near the band center is enhanced. At the same time, in semiconducting tubes the band gap is suppressed. The goal of the present work is to rationalize these properties using the concept of *supersymmetry*.[14] Supersymmetry has a profound effect on the low-energy properties by protecting the states at the band center. We derive a supersymmetric Hamiltonian for and present a simple analytic theory of the above effects. We find that the metallic behavior is protected by the supersymmetry for any magnetic field that is applied perpendicularly to the NT and does not vary along the tube. For a uniform transverse field, in particular, the Fermi velocity in metallic tubes is suppressed by the uniform transverse field as

$$v(B) = v/I_0(x), \quad x = 4\pi R^2 B/\Phi_0, \tag{1}$$

where v is the Fermi velocity for $B = 0$ and $I_0(x)$ is the modified Bessel function. The density of states near the band center is enhanced by the same factor $I_0(x)$. We also calculate the suppression of the gap in semiconducting tubes.

The typical field strength required to make these effects pronounced is quite high. The fields necessary to significantly alter the electron dispersion can be estimated from $\pi R^2 B \simeq \Phi_0 = hc/e$, which gives many tens of tesla even for the tubes of the largest available radii. These fields are not hopelessly strong — they are available, for example, in pulsed magnetic field sources[15] which allow one to reach fields up to $100\,\mathrm{T}$.[16] Because of that and also because of the novel features arising from the supersymmetry and Dirac character of low-energy states, we believe that this problem is sufficiently interesting.

The paper is organized as follows. We first review the basics of the carbon π-electron tight-binding band and its relation with the massless Dirac equation, paying particular attention to coupling to external fields. Then we present a theory of a massless Dirac particle on a cylinder in a transverse magnetic field and calculate the spectrum and density of states. We analyze both the metallic and semiconducting tubes. Then we briefly discuss the behavior in extremely high fields, where a connection can be drawn with the Landau levels and snake states[17] considered previously in the context of the quantum Hall effect.

After that we discuss the effects beyond the Dirac approximation arising from the next order in the gradient expansion of the tight-binding problem. These effects are small but interesting, because they violate supersymmetry and lead to minigaps appearing at the band center.

The effects beyond the Dirac model are controlled by the so-called trigonal warping interaction. We consider it in the presence of a magnetic field and show that its effect depends on the chiral angle and, in particular, is absent for truly metallic armchair nanotubes. These effects have been discussed in Refs.[18,19], using a combination of numerical and analytic methods, for zigzag and armchair tubes. We extend the results of Refs.[18,19] by considering nanotubes with arbitrary chiral angle and also in the presence of minigaps of other origin.

We also discuss the experimental implications of this work. The gap suppression in semiconducting NT's wins over the Zeeman splitting at reasonable fields. We consider the possibility to observe the gap suppression in the tunneling density of states and in the thermally activated transport regime.

Finally, we consider the competition between supersymmetry and electron-electron interactions. We find that although the effect of supersymmetry is reduced by strong interactions, the qualitative features of the spectrum (suppression of the plasmon velocity and of the semimetallic gap) are similar to those of the noninteracting case.

II. DIRAC MODEL FOR THE CARBON π BAND AND NANOTUBES IN EXTERNAL FIELDS

Here we review the basics of the theory of electron states of the two-dimensional (2D) carbon monolayer, making a connection with the 2D Dirac equation. This will provide a good starting point for the following discussion of nanotubes in external fields. We shall start with the tight-binding description of the carbon π band, following the approach of Ref.[20], recall how the Dirac equation arises in this system, and then consider electron coupling to external electromagnetic fields.

The tight-binding Hamiltonian on a honeycomb lattice of carbon atoms with hopping amplitude t between adjacent sites has the form

$$\epsilon\psi(r) = -t \sum_{|r'-r|=a_{cc}} \psi(r') , \qquad (2)$$

where r' are the nearest neighbors of the site r, and a_{cc} is interatomic spacing. In carbon, $t \approx 3\,\text{eV}$ and $a_{cc} = 0.1437\,\text{nm}$. For simplicity and because the electron spectrum is $\epsilon \to -\epsilon$ symmetric, from now on we shall ignore the minus sign in Eq. (2).

The zero chemical potential in Eq. (2) describes the half-filled π band, i.e., the density of one electron per site. For an infinite system, the states of the problem (2) are plane waves and the spectrum is given by $\epsilon(k) = \pm t|\sum_i e^{i\mathbf{k}\cdot\mathbf{r}_i}|$, where $\mathbf{r}_i$ are the nearest-neighbor bond vectors. This is a spectrum of a semimetal with the conduction [$\epsilon(k) > 0$] and valence [$\epsilon(k) < 0$] subbands touching each other at two points K and K' in the Brillouin zone.

The tight-binding bandwidth $6t \simeq 18\,\text{eV}$ is much larger than the energies of the states close to the band center considered below. Because of that, it is useful to project the problem (2) onto the subspace of states with $|\epsilon| \ll t$ and derive an effective low energy Hamiltonian for such states. To carry out the projection, we note that there are only four independent states with $\epsilon = 0$. These states form two complex valued conjugate pairs which we denote as $u(r)$, $v(r)$ and $\bar{u}(r)$, $\bar{v}(r)$. It is convenient to choose the states u and v to be zero on one of the two sublattices of the honeycomb lattice. On the other sublattice each state takes the values 1, $\omega = e^{(2\pi/3)i}$ and $\bar{\omega} = e^{-(2\pi/3)i}$ (see Fig. 1). The states $u(r)$ and $v(r)$ have the same quasimomentum of a value

$$K_0 = \frac{4\pi}{3\sqrt{3}a_{cc}} , \qquad (3)$$

opposite to that of the states $\bar{u}(r)$ and $\bar{v}(r)$. Each pair of states $u(r)$, $v(r)$ and $\bar{u}(r)$, $\bar{v}(r)$ forms a basis at the points K and K', respectively.

Projecting the wave function $\psi(r)$ on $u(r)$ and $v(r)$ and, respectively, on $\bar{u}(r)$ and $\bar{v}(r)$ defines Dirac spinor components for each of the two points K and K'. We focus on the u, v pair and write the states near the point K with small energies $|\epsilon| \ll t$ as linear combinations

$$\psi(r) = \psi_1(r)u(r) + \psi_2(r)v(r), \qquad (4)$$

with the envelope functions $\psi_{1,2}(r)$ varying on the scale much larger than the interatomic spacing a_{cc}. By substituting the wave function (4) in the tight-binding Hamiltonian (2) we have

$$\epsilon\,\psi_1(r) = t\left\{\psi_2(r-a) + \bar{\omega}\psi_2(r-\omega a) + \omega\psi_2(r-\bar{\omega}a)\right\}, \quad (5)$$
$$\epsilon\,\psi_2(r) = t\left\{\psi_1(r+a) + \omega\psi_1(r+\omega a) + \bar{\omega}\psi_1(r+\bar{\omega}a)\right\}, \quad (6)$$

where a is a shorthand notation for a_{cc}. Here the products za with unimodular complex numbers $z = 1, \omega, \bar{\omega}$ in the arguments of $\psi_{1,2}$ are understood in terms of 2D rotations of the vector $a\hat{\mathbf{x}}$ by $\arg z$.

Expanding slowly varying $\psi_{1,2}(r)$, we obtain

$$\begin{aligned} \epsilon\psi_1(r) &= -\hbar v(\partial_x - i\partial_y)\psi_2(r), \\ \epsilon\psi_2(r) &= \hbar v(\partial_x + i\partial_y)\psi_1(r), \end{aligned} \qquad (7)$$

where $v = \frac{3}{2}t\,a_{cc}/\hbar$. The Hamiltonian (7) defines massless Dirac fermions with the linear spectrum $\epsilon(k) = \pm\hbar v|\mathbf{k}|$. In carbon, the velocity $v = 8 \times 10^7\,\text{cm/s}$. Similar relations hold for the point K'.

Equations (7) can be cast in the conventional Dirac form $\epsilon\psi = \mathcal{H}\psi$ with

$$\mathcal{H} = v\,\alpha\cdot\mathbf{p} = v\,(\alpha_1 p_1 + \alpha_2 p_2) \qquad (8)$$

for the two-component wave function $\psi = (\psi_1, \psi_2)^{\text{T}}$, with $\alpha_{1,2}$ given by the Pauli matrices:

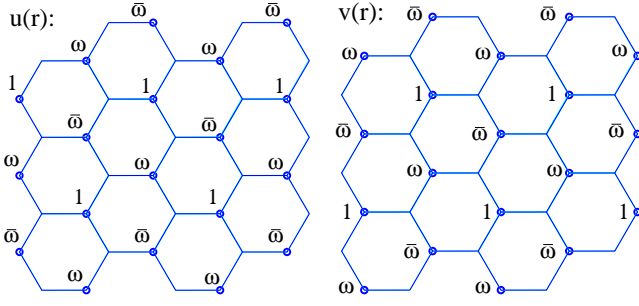$$\alpha_1 = \sigma_2 , \quad \alpha_2 = -\sigma_1 . \qquad (9)$$

FIG. 1: Shown are two plane-wave basis states $u(r)$ and $v(r)$ of the problem (2) with $\epsilon = 0$. Both $u(r)$ and $v(r)$ take the values 1, $\omega = e^{(2\pi/3)i}$ and $\bar{\omega} = e^{-(2\pi/3)i}$ on one sublattice and vanish on the other sublattice of the honeycomb lattice. The states $u(r)$ and $v(r)$ have the same quasimomentum and form a basis of the Dirac problem (9) at the point K. The independent basis states at the point K' are $\bar{u}(r)$ and $\bar{v}(r)$.

The Hamiltonian near the K' point can be derived in a similar way. The result has the form (8) with a sign change in the second term: $\alpha_1 = \sigma_2$, $\alpha_2 = \sigma_1$.

Below we shall consider electrons in the presence of external electromagnetic fields. The minimal form of the coupling to external fields follows from the gauge invariance:

$$\mathcal{H} = v\,\alpha \cdot \left(\mathbf{p} - \frac{e}{c}\mathbf{A}\right) + e\varphi \ , \qquad (10)$$

where φ and $\mathbf{A}$ are the scalar and vector electromagnetic potentials. The effect of electron spin, ignored here for simplicity, can be included in Eq. (10) via a Zeeman term.

Equation (10) describes the lowest-order approximation in the gradients of $\psi_{1,2}$ and the potentials φ and $\mathbf{A}$. Here we consider the exact tight-binding equations in the presence of external fields:

$$\epsilon\,\psi_1(r) = t\left(\sum_{z=1,\omega,\bar{\omega}} \bar{z}\,e^{i\gamma_{r,\,r-za}}\psi_2(r-za)\right), \qquad (11)$$

$$\epsilon\,\psi_2(r) = t\left(\sum_{z=1,\omega,\bar{\omega}} z\,e^{i\gamma_{r,\,r+za}}\psi_1(r+za)\right), \qquad (12)$$

where the phases $\gamma_{r,r'}$ are the integrals of the vector potential along the nearest-neighbor bonds,

$$\gamma_{r,r'} = \frac{2\pi}{\Phi_0}\int_{r'}^{r} \mathbf{A}(\mathbf{x})\cdot d\mathbf{l}\ . \qquad (13)$$

Equations (11) and (12) can be used to obtain the gradient terms of higher order along with the coupling to external fields. One can check that expanding the exponents in Eqs. (11) and (12) and keeping the lowest nonvanishing terms gives the Dirac Hamiltonian (10). In Sec. VI we shall use Eqs. (11) and (12) to obtain higher-order corrections to Eq. (10).

To apply the above results to nanotubes, we consider electrons on a carbon sheet rolled into a cylinder. The transformation of the tight-binding problem (2) to the Dirac problem (7) based on the representation (4) is valid provided that the cylinder circumference $L = 2\pi R$ is much larger than the interatomic spacing $a_{\rm cc}$. Since for typical NT radii the ratio $L/a_{\rm cc}$ can be between 10 and 20, the approximation (4) is entirely adequate.

The NT electron properties, depending on the nanotube structure, can be either metal like or dielectric like. Which of these situations takes place depends on the manner the cylinder is obtained from the carbon monolayer. In the Dirac approach, the condition for metallic behavior can be formulated directly in terms of the functions $u(r)$ and $v(r)$: The nanotube is metallic *if and only if* one can define on the NT cylinder the two functions $u(r)$ and $v(r)$ according to Fig. 1 without running into a mismatch of the function values upon the cylinder closure.

To demonstrate this, let us suppose that the functions $u(r)$ and $v(r)$ on the cylinder exist. Without loss of generality we choose the x axis along the cylinder and the y axis along the circumference. The problem (7) has periodic boundary conditions in the y direction, and thus the wave functions can be factorized as $\psi_{1,2}(r) = \psi_{1,2}(x)e^{ik_n y}$, where $k_n = 2\pi n/L = n/R$. Then the dispersion relation for the 1D problems describing motion along the x axis with fixed k_n is

$$\epsilon_n(k_x) = \pm\hbar v(k_x^2 + k_n^2)^{1/2}\ . \qquad (14)$$

In this case the subband with $n = 0$ has metallic properties and the subbands with $n \neq 0$ are dielectric.

Now let us consider the other possibility when the cylinder is constructed in such a way that the functions $u(r)$ and $v(r)$ cannot be defined without a value mismatch. In this case, upon rolling the carbon sheet into a cylinder, the sites with different function values shown in Fig. 1 are glued together. However, since all values of the functions $u(r)$ and $v(r)$ are powers of $\omega = e^{(2\pi/3)i}$, one notes that Eqs. (7) can still be used here if they are augmented with *quasiperiodic* boundary conditions, $\psi_{1,2}(x, y+L) = \omega\psi_{1,2}(x,y)$ or $\psi_{1,2}(x, y+L) = \bar{\omega}\psi_{1,2}(x,y)$, which, combined with the value mismatch of $u(r)$ and $v(r)$, make $\psi(r)$ single valued. Factoring the wave function as above, one obtains 1D subbands with the dispersion of the form (14), in this case with $k_n = (n \pm \frac{1}{3})/R$. Note that in this case all spectral branches have dielectric character.

Now we consider a nanotube in the presence of a *parallel* external magnetic field. In this case, electron properties are described by the Dirac equation (10) with $\varphi = 0$ and the vector potential $\mathbf{A}$ with just the y component, $A_y = \Phi/L$, where $\Phi = \pi R^2 B$ is the magnetic flux. The boundary conditions in the y direction are periodic for the metallic case and quasiperiodic for the dielectric case. In the presence of a parallel magnetic field the problem remains separable and thus the wave function can be factorized in just the same way as above. One again finds

1D subbands with the spectrum (14), where

$$k_n R = \begin{cases} n + \phi_\parallel \,, & \text{metallic,} \\ n \pm \frac{1}{3} + \phi_\parallel & \text{semiconducting,} \end{cases} \quad (15)$$

for the metallic and semiconducting NT's, respectively, with $\phi_\parallel = \Phi/\Phi_0$ and $\Phi_0 = hc/e$. Thus in the presence of a parallel field the gapless $n = 0$ branch of the metallic nanotube spectrum (14) acquires a gap.[7,19] Interestingly, there is no threshold for this effect, since the gap forms at arbitrarily weak field. The gap size is $2\Delta = 2|\phi_\parallel|\hbar v/R$. One notes that the field-induced gap appears not at the Fermi level but at the center of the electron band. Thus it affects the metallic NT properties only for electron density sufficiently close to half-filling.

III. DIRAC EQUATION AND SUPERSYMMETRY

At the energies smaller than the total bandwidth $6t$ (ca. $18\,\text{eV}$ in carbon) electron states are described (separately near each of the K and K' points) by the massless Dirac equation (10). For a uniform transverse magnetic field, the field component normal to the NT surface is $B_\perp(\theta) = B\sin\theta$, where $\theta = y/R$ is the azimuthal angle. The corresponding vector potential can be chosen along the tube axis x, $\mathbf{A}(\mathbf{r}) = \hat{x}A(\theta)$, where

$$\frac{eR}{\hbar c} A(\theta) = 2\phi\cos\theta \,, \quad \phi \equiv \frac{\pi R^2 B}{\Phi_0} \,. \quad (16)$$

In this case the longitudinal momentum $\hbar k$ is conserved and the states on the NT cylinder have a plane-wave form $\psi(r) = \psi(x,\theta) = \psi(\theta)e^{ikx}$. The Dirac Hamiltonian for $\psi(\theta)$ is

$$\mathcal{H}_D = \Delta_0 \left\{ i\sigma_1\partial_\theta + (kR - 2\phi\cos\theta)\,\sigma_2 \right\}, \quad (17)$$

with $\sigma_{1,2}$ the Pauli matrices and

$$\Delta_0 = \frac{\hbar v}{R} \,. \quad (18)$$

The equations near the K' point have the form (17) with a sign change in the first term, $\sigma_1 \to -\sigma_1$.

The eigenvalues of the operator (17) give the electron dispersion relation $\epsilon(k)$. We have chosen the dimensionless transverse field parameter ϕ in the form (16), which makes contact with the parallel field problem,[7,19] Eq. (15).

The NT states are described by quasiperiodic wave functions on the cylinder ($y = R\theta$),

$$\psi(y + L) = e^{2\pi i\delta}\psi(y) \,, \quad L = 2\pi R \,, \quad (19)$$

with

$$\delta = \begin{cases} 0 \,, & \text{metallic,} \\ \pm\frac{1}{3} & \text{semiconducting,} \end{cases} \quad (20)$$

We consider the problem (17) with an arbitrary phase δ in the boundary conditions (19). This will permit us to generalize the results to the cases of metallic NT's with a minigap induced by curvature[21] or in the presence of a parallel magnetic field. These problems can be described using the boundary conditions (19) with δ slightly shifted away from the ideal values (20).

The electron bands $\epsilon(k)$ can be studied using the transfer matrix. We integrate the Dirac equation in the interval $0 < \theta < 2\pi$ and write a formal solution $\psi(\theta)$ to the problem $\mathcal{H}_D\psi = \epsilon\psi$ as $\psi(\theta) = S(\theta)\psi(0)$ with the 2×2 matrix

$$S(\theta) = \mathcal{T}\exp\int_0^\theta \left\{ -i\tilde\epsilon\,\sigma_1 + (2\phi\cos\theta' - kR)\,\sigma_3 \right\} d\theta' \,, \quad (21)$$

where $\tilde\epsilon = \epsilon/\Delta_0$. Here $\mathcal{T}$ stands for operator ordering with respect to θ. The quasiperiodic boundary condition (19) requires

$$\text{tr}\,S_{\theta=2\pi} = 2\cos(2\pi\delta) \,. \quad (22)$$

Different energy bands $\epsilon = \epsilon_n(k)$ can be found numerically as solutions of Eq. (22). The bands obtained in this way are displayed in Fig. 2.

In the present section we show that supersymmetry allows one to make rather general statements about the low-energy NT spectrum. Originally, supersymmetry was suggested[22] as a special symmetry between the bosonic and fermionic sectors of relativistic field theories that protects the zero-energy eigenstate. Later, the concept of supersymmetry was brought to single-particle quantum mechanics.[23] This has yielded the classification of exactly solvable potentials using factorization of the Schrödinger equation (see Ref.[14] for a review).

Below we apply the arguments of supersymmetry to a problem of NT electrons in a generic magnetic field $\mathbf{B}(\mathbf{r})$ that (i) is perpendicular to the NT axis and (ii) does not vary along the NT. In this case the field component normal to the NT surface is a function only of $y = R\theta$, $B_\perp \equiv B(y)$. Similarly to Eq. (16), we choose the following gauge:

$$A_x \equiv A(y) = \frac{\Phi_0}{2\pi}\frac{d\varphi}{dy} \,, \quad A_y = 0 \,, \quad (23)$$

where

$$\frac{d^2\varphi}{dy^2} = -\frac{2\pi}{\Phi_0} B(y) \,. \quad (24)$$

The function $\varphi(y)$ is uniquely defined by demanding periodicity

$$\varphi(y + L) = \varphi(y) \quad (25)$$

and zero average

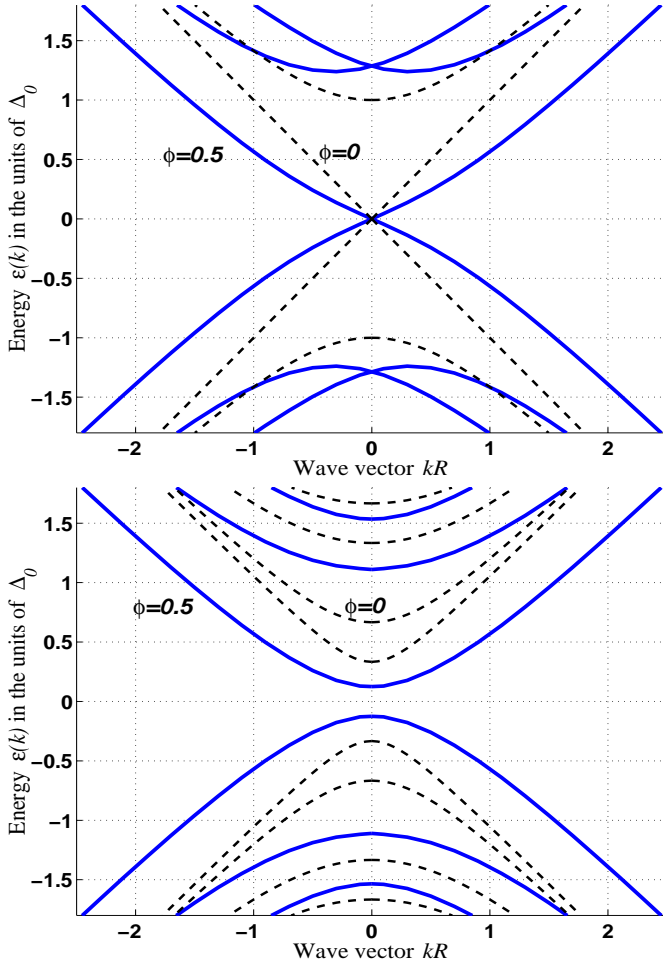$$\int_0^L dy\,\varphi = 0 \,. \quad (26)$$

FIG. 2: Electron dispersion $\epsilon(k)$ in the presence of a large uniform transverse magnetic field $\phi = 0.5$ (bold lines) and in the absence of the field (dashed lines). *Top:* metallic NT ($\delta = 0$). No gap opens due to supersymmetry, but the velocity is suppressed according to Eq. (45). *Bottom:* semiconducting case ($\delta = 1/3$). The energy gap is suppressed by the factor $g_{1/3}(\phi)$; see Eq. (58) and Fig. 4.

The corresponding Dirac Hamiltonian reads

$$\tilde{\mathcal{H}}_D = \hbar v \left\{ i\sigma_1 \partial_y + \left(k - \frac{d\varphi}{dy} \right) \sigma_2 \right\} , \qquad (27)$$

which reduces to Eq. (17) when $B(y) = B\sin(y/R)$. It is useful to decompose $\tilde{\mathcal{H}}_D$ into two pieces,

$$\tilde{\mathcal{H}}_D = Q + Q^\dagger, \qquad (28)$$

where

$$Q \equiv \begin{pmatrix} 0 & 0 \\ \mathcal{A} & 0 \end{pmatrix}, \quad Q^\dagger \equiv \begin{pmatrix} 0 & \mathcal{A}^\dagger \\ 0 & 0 \end{pmatrix} \qquad (29)$$

and

$$\mathcal{A} \equiv \hbar v \left\{ i\partial_y + i \left(k - \frac{d\varphi}{dy} \right) \right\},$$

$$\mathcal{A}^\dagger \equiv \hbar v \left\{ i\partial_y - i \left(k - \frac{d\varphi}{dy} \right) \right\}. \qquad (30)$$

The connection with the supersymmetric quantum mechanics (see Chap. 2 in Ref.[14]) is established by constructing a supersymmetric Hamiltonian

$$\mathcal{H}_{\mathrm{SUSY}} \equiv \begin{pmatrix} \mathcal{A}^\dagger \mathcal{A} & 0 \\ 0 & \mathcal{A}\mathcal{A}^\dagger \end{pmatrix}, \qquad (31)$$

which, together with Q and $Q^\dagger$, satisfies the superalgebra $sl(1/1)$,

$$[\mathcal{H}_{\mathrm{SUSY}}, Q] = [\mathcal{H}_{\mathrm{SUSY}}, Q^\dagger] = 0,$$
$$\{Q, Q^\dagger\} = \mathcal{H}_{\mathrm{SUSY}}, \quad \{Q, Q\} = \{Q^\dagger, Q^\dagger\} = 0. \qquad (32)$$

Here $\{A, B\} = AB + BA$ stands for anticommutator of operators. In relativistic field theories, the *supercharges* Q and $Q^\dagger$ transform fermionic and bosonic degrees of freedom into each other. Although we deal with a single electron NT spectrum, one could *formally* interpret the upper and lower components of the wave function ψ as fermionic and bosonic sectors of the supersymmetric Hamiltonian $\mathcal{H}_{\mathrm{SUSY}}$.

One interesting implication of the algebra (32) is that $\mathcal{H}_{\mathrm{SUSY}}$ can be expressed as sums of the square of Hermitian supercharges, Q_1 and Q_2,

$$\mathcal{H}_{\mathrm{SUSY}} = Q_1^2 + Q_2^2, \qquad (33)$$

where

$$Q_1 \equiv \frac{1}{\sqrt{2}} \left(Q + Q^\dagger \right) , \quad Q_2 \equiv \frac{i}{\sqrt{2}} \left(Q - Q^\dagger \right). \qquad (34)$$

From Eq. (29), one verifies $Q_1^2 = Q_2^2$ and

$$\mathcal{H}_{\mathrm{SUSY}} = 2Q_1^2 = \tilde{\mathcal{H}}_D^2. \qquad (35)$$

Thus the energy spectra of $\mathcal{H}_{\mathrm{SUSY}}$ and $\tilde{\mathcal{H}}_D$ are closely related.

Let us now show how supersymmetry protects zero-energy states of $\mathcal{H}_{\mathrm{SUSY}}$ and $\tilde{\mathcal{H}}_D$. For that, we construct zero energy states of $\mathcal{H}_{\mathrm{SUSY}}$ that are compatible with the boundary condition (19). Due to Eq. (33), any such state ψ satisfies

$$Q_1\psi = Q_2\psi = 0 \qquad (36)$$

or, equivalently,

$$Q\psi = Q^\dagger\psi = 0 . \qquad (37)$$

The latter equation has two independent solutions

$$\psi_1 = e^{-ky+\varphi(y)} \begin{pmatrix} 1 \\ 0 \end{pmatrix} , \quad \psi_2 = e^{ky-\varphi(y)} \begin{pmatrix} 0 \\ 1 \end{pmatrix} . \qquad (38)$$

Note that since k is real and $\varphi(y)$ is periodic in y, the zero-energy solutions (38) are compatible with the boundary condition (19) *if and only if* $\delta = 0$ and $k = 0$.

For the latter case the exact zero-energy eigenstates of $\tilde{\mathcal{H}}_D$ can be written as

$$\psi_1^{(0)} = \frac{e^{\varphi(y)}}{\sqrt{Lg_0^{(1)}}}\begin{pmatrix} 1 \\ 0 \end{pmatrix} , \quad \psi_2^{(0)} = \frac{e^{-\varphi(y)}}{\sqrt{Lg_0^{(2)}}}\begin{pmatrix} 0 \\ 1 \end{pmatrix} , \quad (39)$$

where normalization requires

$$Lg_0^{(1)} = \int_0^L dy\, e^{2\varphi(y)} , \quad Lg_0^{(2)} = \int_0^L dy\, e^{-2\varphi(y)} . \quad (40)$$

In the case of a uniform perpendicular field

$$\varphi = 2\phi\sin\theta , \quad \theta = y/R , \quad (41)$$

the normalization factors are given by the modified Bessel function:

$$g_0^{(1)} = g_0^{(2)} = \frac{1}{2\pi}\oint e^{4\phi\sin\theta}d\theta = I_0(4\phi) . \quad (42)$$

The states (39) are degenerate at any field strength.

Let us stress here that the zero-energy eigenstates (39) of $\tilde{\mathcal{H}}_D$ exist[24] at $\delta = 0$, $k = 0$ for a generic magnetic field perpendicular to the NT and not varying along the tube. An example is a field of a current flowing along the wire parallel to the nanotube axis. Moreover, the above arguments still apply if the NT does not have a circular cross section, as long as the minigap due to the curvature[2,3] of the graphene sheet is not open. In what follows we confine ourselves to the case of a cylindrical NT in a homogeneous perpendicular magnetic field for simplicity, bearing in mind the generalizations mentioned above.

Using the states (39) one can study how the linear dispersion relation changes near the band center $\epsilon = 0$. For that we project the Hamiltonian (17) onto the basis

$$\psi_{1,2}(x,\theta) = e^{ikx}\psi_{1,2}^{(0)}(\theta) . \quad (43)$$

The projected Hamiltonian

$$\mathcal{H}_D|_{\Psi_{1,2}} = \hbar k\bar{v}\,\sigma_2 , \quad \bar{v} = \frac{v}{I_0(4\phi)}, \quad (44)$$

yields the dispersion relation

$$\epsilon(k) = \pm\hbar k\left(\frac{v}{I_0(4\phi)}\right) . \quad (45)$$

This describes a *reduction* of the Fermi velocity $\hbar^{-1}d\epsilon/dk$ near $\epsilon = 0$ by a factor $I_0(4\phi)$. Since $I_0(4\phi) > 1$, the density of states at the band center,

$$\nu = dN/d\epsilon = \frac{4}{\pi\hbar v}I_0(4\phi), \quad (46)$$

is *enhanced*. (The factor of 4 accounts for the spin and valley degeneracy neglecting the Zeeman splitting; see Sec. IV below.) Due to the exponential behavior of the Bessel function in Eq. (45) at large ϕ, this enhancement
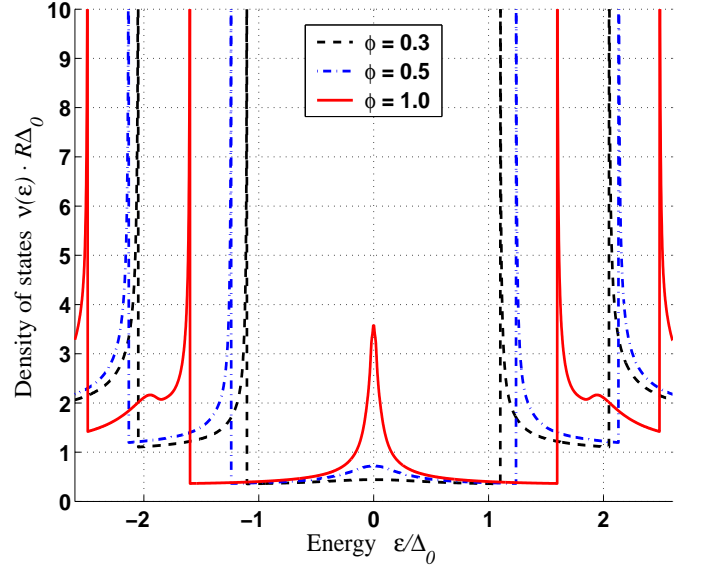

FIG. 3: Density of states $\nu = dN/d\epsilon$ in metallic NT's per one fermion flavor as a function of energy in the units of $\Delta_0 = \hbar v/R$. The peak value $\nu(0)$ at the band center is given by Eq. (46).

becomes dramatic at high fields (Fig. 3). The reduction of the Fermi velocity and the corresponding density-of-states enhancement is a general consequence of a supersymmetry. Indeed, in the generic field case described above the velocity is reduced by a factor $\sqrt{g_0^{(1)}g_0^{(2)}} \geq 1$. Both $g_0^{(1)}$, $g_0^{(2)} \geq 1$ [see Eq. (40)] since the average of an exponential is greater than or equal to an exponential of the average.

In the single-particle approximation, the tunneling density of states coincides with the thermodynamic density of states (46). The peak in the tunneling density of states at the band center is a distinct manifestation of supersymmetry. Recently, a scanning tunneling probe has been used[6] to study curvature-induced minigaps in nominally metallic tubes placed on a metallic substrate. In this setup, the electron interactions that could have modified the single-particle behavior are screened by the substrate, and the measured density of states is unaffected by Luttinger liquid effects. In a similar system in a high transverse field, an enhancement of tunneling at the band center, Eq. (46), and a peak in the density of states (Fig. 3) are the experimental signatures to look for.

IV. GAP SUPPRESSION

In the present section we consider nanotubes that have a gap Δ at the band center. We characterize them by the parameter $|\delta| = \Delta/\Delta_0$ that enters the boundary condition (19). There are two kinds of such tubes: semiconducting NT's with $\delta = \pm 1/3$ and nominally metallic NT's

in which a minigap appears due to curvature or external field, yielding a small $|\delta| \ll 1$. The Dirac problem (17) and (19) is not supersymmetric for $\delta \neq 0$. However, since the supersymmetry is an exact property at $\delta = 0$, one can still expect it to manifest itself in a problem with a relatively small δ. Below we show that a gap at the band center is *suppressed* in the presence of an external transverse field:

$$\Delta(\phi) = \frac{\Delta}{g_\delta(\phi)} , \quad g_\delta(\phi) > 1 , \qquad (47)$$

where the gap suppression factor $g_\delta(\phi)$ diverges as $\phi \rightarrow \infty$. This means that supersymmetry is restored in the limit of a strong field. The suppression of the gap in semiconducting NT's is illustrated in Fig. 2 (lower panel).

We shall first consider a simpler case of a nominally metallic tube with $\delta \ll 1$. The gap in this case can be found using perturbation theory in δ. For that, we perform a gauge transformation $\psi(\theta) \rightarrow e^{i\delta\theta}\psi'(\theta)$ and for $\psi'(\theta)$ obtain a problem with the *periodic* boundary condition. The new Hamiltonian differs from Eq. (17) by a term linear in δ:

$$\mathcal{H}' = \mathcal{H}_D - \delta\Delta_0\sigma_1 . \qquad (48)$$

It is convenient to rewrite this Hamiltonian as

$$\mathcal{H}' = \mathcal{H}_D^{(0)} + \Delta_0(kR\,\sigma_2 - \delta\sigma_1) , \qquad (49)$$

where $\mathcal{H}_D^{(0)}$ is the Hamiltonian (17) with $k = 0$. We note that $\mathcal{H}_D^{(0)}$ is a supersymmetric Hamiltonian with eigenstates (39). The spectrum of the Hamiltonian $\mathcal{H}'$ at small kR and δ can be found by projecting the second term of Eq. (49) on the basis (43) of plane-wave states constructed out of Eq. (39). This yields the dispersion relation

$$\epsilon(k) = \pm\frac{\Delta_0}{I_0(4\phi)} \left[(kR)^2 + \delta^2\right]^{1/2} . \qquad (50)$$

Thus we find that in this case the gap is suppressed by the same factor (42),

$$g_0(\phi) = I_0(4\phi) > 1, \qquad (51)$$

as the Fermi velocity in metallic NT's. The gap suppression is described by Eq. (51) in the limit of small δ for any magnetic field ϕ.

One can also study the gap suppression analytically for generic δ using perturbation theory in the field ϕ. The energy $\epsilon(k = 0)$ that gives the gap is defined by the condition (22) for the transfer matrix. We calculate the trace of the transfer matrix (21) at $k = 0$ by expanding it perturbatively in $\phi \ll 1$:

$$\text{tr } S_{\theta=2\pi} = 2\cos 2\pi\bar\epsilon + 8\lambda_1\,\phi^2 + 32\lambda_2\,\phi^4 + \mathcal{O}(\phi^6), \quad (52)$$

where $\tilde\epsilon = \epsilon(0)/\Delta_0$ and the coefficients $\lambda_{1,2}$ are given by

$$\lambda_1 = -\frac{2\pi\tilde\epsilon\,\sin 2\pi\tilde\epsilon}{1 - 4\tilde\epsilon^2} , \qquad (53)$$

$$\lambda_2 = -\pi\tilde\epsilon\,\frac{2\pi\tilde\epsilon\left(1 - 4\tilde\epsilon^2\right)\cos 2\pi\tilde\epsilon + \left(\frac{1}{2} + 6\tilde\epsilon^2\right)\sin 2\pi\tilde\epsilon}{\left(1 - 4\tilde\epsilon^2\right)^3} \quad (54)$$
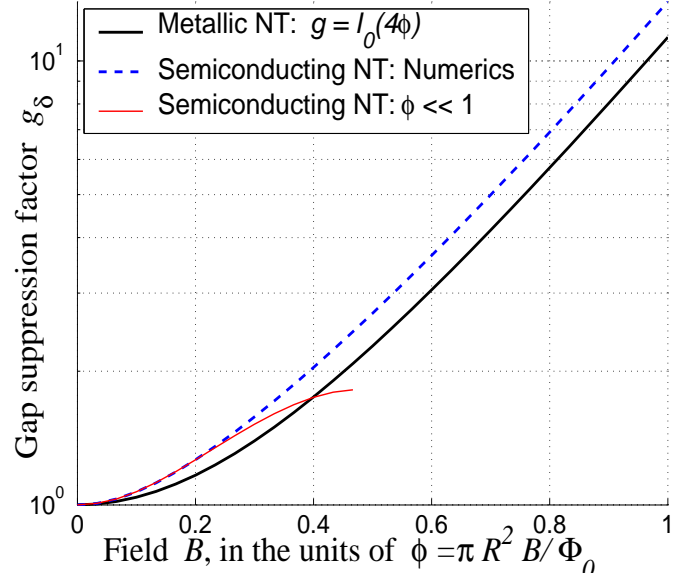

FIG. 4: Gap suppression factors (47) for nominally metallic NT's, $\delta = 0$ (solid line), and semiconducting NT's, $\delta = 1/3$ (dashed line), as a function of field ϕ. The fine solid line is the result of the expansion (58) in powers of ϕ. (Note the logarithmic scale for g_δ.)

The condition (22) on the energy along with the definition of the suppression factor (47) gives

$$g_\delta = 1 + \alpha_\delta\phi^2 + \beta_\delta\phi^4 + \mathcal{O}(\phi^6) , \qquad (55)$$

$$\alpha_\delta = \frac{4}{1 - 4\delta^2} , \quad \beta_\delta = 4\frac{1 - 20\delta^2}{\left(1 - 4\delta^2\right)^2} . \qquad (56)$$

Substituting, in Eq. (56), $\delta = 0$ and $\delta = 1/3$ we obtain

$$g_0(\phi) = 1 + 4\phi^2 + 4\phi^4 + \mathcal{O}(\phi^6) \quad \text{(metallic)} , \qquad (57)$$

$$g_{1/3}(\phi) = 1 + \frac{36}{5}\phi^2 - \frac{396}{25}\phi^4 + \mathcal{O}(\phi^6) \quad \text{(semiconducting)} \quad (58)$$

The expression (57) coincides with the Taylor expansion of $I_0(4\phi)$.

These analytical results can be compared with the gap suppression factors obtained numerically (Fig. 4). For nominally metallic NT's with small minigap we find that at $\delta \ll 1$ the value $g_{\delta\rightarrow 0}$ is accurately given by Eq. (51). The analytical expression (51) coincides with the numerics in the entire field range. In the semiconducting case of $\delta = 1/3$ the expansion (58) works reasonably well at $\phi \leq 1/4$. At larger fields $\phi > 1/4$ the gap is suppressed exponentially, $g_{1/3}(\phi) \propto e^{4\phi}$ (see Fig. 4).

Let us discuss the possibilities to observe the suppression of the gap. A competing effect due to the magnetic field that leads to a gap suppression is the Zeeman spin coupling $\mathcal{H}_Z = -\mu\sigma B$ with $\mu = e\hbar/2mc$. The gap suppression at weak fields, $\phi \ll 1$, with the Zeeman effect included, is described by

$$\Delta(\phi) = \Delta - \alpha_\delta\phi^2\Delta - \mu B, \qquad (59)$$

with α_δ given by Eq.(56). The Zeeman effect, linear in B, dominates at weak fields. However, the orbital effect $\alpha_\delta \phi^2 \Delta$, quadratic in B, overcomes the Zeeman effect at relatively moderate fields $\phi \ll 1$.

For semiconducting NT's the gap $\Delta = \hbar v/3R$, and Eq. (56) gives $\alpha_{1/3} = 36/5$. In this case, the inequality $\alpha_{1/3}\phi^2\Delta > \mu B$ yields $\phi > 1.13\,a_B/R$ with $a_B = \hbar^2/me^2$ the Bohr radius. Using carbon parameters we estimate that the magnetic field has to exceed

$$B_0 = 78\,(R\,[\mathrm{nm}])^{-3}\ \ \mathrm{T} \tag{60}$$

which can be low enough for tubes of large radius.

The energy gap can be studied experimentally by measuring transport in the thermally activated regime. The thermal activation energy will depend on the magnetic field according to Eq. (59). The resistance

$$R(T) \propto \exp[\Delta(\phi)/k_{\mathrm{B}}T] \tag{61}$$

will be sensitive to magnetic field because the variation of the gap can exceed $k_{\mathrm{B}}T$ even at the fields much smaller than Eq. (60). For example, consider a NT of radius $R = 1\,\mathrm{nm}$, in which case $\Delta = \hbar v/3R = 0.178$ eV. For the magnetic field $B = B_0$ from Eq. (60) we have $\phi = 0.060$ and $\alpha_{1/3}\phi^2 = 0.026$. In this case the gap shift $\alpha_{1/3}\phi^2\Delta = 4.6\,\mathrm{meV}$ is larger than $k_{\mathrm{B}}T$ at $T < 53\,\mathrm{K}$.

V. ELECTRON SPECTRUM IN EXTREMELY LARGE FIELDS

Below we consider the qualitative features of the energy bands in metallic NT's in the limit of a large uniform external field, corresponding to $\phi \geq 1$. The behavior of the band dispersion at $|k|R \ll \phi$ can be attributed to the Landau levels of the problem (17). Let us consider a square of the Hamiltonian (17) and the eigenvalue problem $\mathcal{H}_D^2\psi = \epsilon^2\psi$. It reads

$$\mathcal{H}_D^2\psi = \Delta_0^2[-\partial_\theta^2 + U_k(\theta)]\psi = \epsilon^2(k)\,\psi\ , \tag{62}$$
$$U_k(\theta) = (2\phi\cos\theta - kR)^2 - 2\phi\sigma_3\sin\theta\ , \tag{63}$$

with $\psi(\theta)$ obeying the boundary conditions (19). Note that $\mathcal{H}_D^2$ is a diagonal 2×2 matrix in the space of spinors ψ. In what follows we take $\sigma_3 = +1$.

When $\phi \gg 1$, the kinetic energy of Eq. (62) is frozen since $U_k(\theta) \propto \phi^2$ is much greater than ∂_θ^2. In this limit, the Hamiltonian is dominated by the potential energy term $U_k(\theta)$ and the low-energy states are localized near the minima of $U_k(\theta)$. At $\phi \gg 1$ the potential $U_k(\theta)$ has two slightly asymmetric minima near $\theta_\pm = \pm\pi/2$, where it can be approximated by a harmonic potential $U_k(\theta) \approx \mp 2\phi + 4\phi^2(\theta - \theta_\pm)^2$. The size of electronic wave function in the circumferential direction is

$$w \simeq l_B = R/\sqrt{2\phi} \ll R\ , \tag{64}$$

where $l_B = (\hbar c/eB)^{1/2}$ is the magnetic length. Thus at large field the electrons are localized near the extrema

of the magnetic field $\theta_\pm$. In these regions the field is approximately constant: $|B_\perp(\theta)| \approx B$.

The Landau level spectrum $\epsilon_n^2(k)$ of Eq. (62) obtained within the harmonic approximation yields approximately k-independent levels for $\mathcal{H}_D$:

$$\epsilon_n(kR \ll \phi) = \pm 2\,\Delta_0\,\sqrt{n|\phi|}\ , \quad n = 0, 1, 2, \dots\ . \tag{65}$$

The lowest-energy level of Eq. (62) is $\epsilon = 0$ at $k = 0$. This value, because of the supersymmetry, is not approximate but exact.

The behavior at large momenta $|k|R \gg \phi$ can be understood semiclassically in terms of the so-called *snake states*.[17] Snake states correspond to a classical particle moving along zero-field lines. This motion is stable for a particle traveling in one direction and is unstable for it traveling in the opposite one. The snake states are located at $\theta = 0$ and $\theta = \pi$, where the field $B(\theta) = B\sin\theta$ vanishes. This is consistent with the high-field limit of the problem (62), since at $|k|R \gg \phi$ the minimum of $U_k(\theta)$ is $\theta_0 \approx 0$ for $kB > 0$ and $\theta_0 \approx \pi$ for $kB < 0$. The dispersion relation for such states is

$$\epsilon(k) = \pm\Delta_0\sqrt{U_k(\theta_0)} \approx \pm\hbar v(|k| - 2|\phi|/R)\ . \tag{66}$$

This linear dispersion relation with an offset $2|\phi|\,\hbar v/R$ holds even for small fields as long as $|k|R \gg \max\{\phi, 1/\phi\}$ (see Fig. 2, large kR).

Since θ_0 is different for positive and negative k, the left- and right-moving snake states are spatially separated. For $\phi > 0$, for instance, the left- (right-) moving snake states are localized near $\theta = \pi$ ($\theta = 0$). The characteristic width of the snake-state wave function is

$$w_{\mathrm{snake}} = l_B^{1/2}(R/k)^{1/4} \propto |\nabla B|^{-1/4}\ . \tag{67}$$

The width $w_{\mathrm{snake}} \ll R$ when $kR \gg 1/|\phi|$. In the Dirac problem the wave function width (67) is different from that for the Schrödinger problem discussed in Ref.[17], where $w_{\mathrm{snake}} \propto |\nabla B|^{-1/2}$.

VI. BEYOND THE DIRAC EQUATION: SUPERSYMMETRY BREAKING

The two effects considered in Secs. III and IV—the density of states enhancement at $\epsilon = 0$ in metallic NT's and the suppression of the energy gap in semiconducting NT's—are manifestations of the supersymmetry of the low-energy Dirac Hamiltonian (17). However, supersymmetry is not present in the original tight-binding problem (2). Below we show that the terms correcting Eq. (17) in the next order of the gradient expansion violate supersymmetry. Thus the supersymmetry in nanotubes is not exact but approximate: the nonsupersymmetric effects are small in a_{cc}/R.

To obtain the nonsupersymmetric terms of the effective Hamiltonian we consider the low-energy subspace of states with $|\epsilon| \ll t$ near the Dirac points K and K'. The

basis states at $\epsilon = 0$ are the functions $u(r)$, $v(r)$ and $\bar{u}(r)$, $\bar{v}(r)$ defined in Sec. II (see Fig. 1). The wave function near the point K (K') can be represented as a linear superposition (4) of $u(r)$ and $v(r)$ [respectively, $\bar{u}(r)$ and $\bar{v}(r)$] multiplied by the smooth envelope functions $\psi_{1,2}(r)$. We perform a gradient expansion of the slowly varying envelope functions using Eq. (11). In the lowest nonvanishing order in $a_{cc}\partial\psi_{1,2}$ we retain the Hamiltonian (17) with $v = 3ta_{cc}/2\hbar$.

The terms of second order in the gradients $a_{cc}^2 \partial_i \partial_j \psi_{1,2}$ give the required correction $\mathcal{H}_{tw}$ to the Dirac Hamiltonian $\mathcal{H}_D$ called the carbon *trigonal warping* interaction. In this case, since we are interested in the problem in an external field, the gradient expansion of Eq. (11) should be accompanied by an expansion of the phase factors (13). After this expansion is carried out we choose the tube axis orientation with respect to the carbon lattice by specifying the chiral angle Θ. The full Hamiltonian $\mathcal{H}_{tot}$ obtained in such a way for NT's has the form

$$\mathcal{H}_{tot} = e^{i(\Theta/2)\sigma_3}\mathcal{H}_D e^{-i(\Theta/2)\sigma_3} + e^{-i\Theta\sigma_3}\mathcal{H}_{tw}e^{i\Theta\sigma_3} , \quad (68)$$

where $\mathcal{H}_D$ is the Dirac Hamiltonian (17) and the trigonal warping interaction $\mathcal{H}_{tw}$ is given by

$$\mathcal{H}_{tw} = -\frac{a_{cc}}{4R}\Delta_0\left\{\left(\kappa^2 + \partial_\theta^2\right)\sigma_1 + i\left(2\kappa\,\partial_\theta + \frac{d\kappa}{d\theta}\right)\sigma_2\right\}, \quad (69)$$

where

$$\kappa(\theta) \equiv kR - \frac{eR}{\hbar c}A(\theta) . \quad (70)$$

The term $\mathcal{H}_{tw}$ breaks the supersymmetry of the Hamiltonian $\mathcal{H}_{tot}$. Thus we expect the zero-energy state to disappear. Note that $\mathcal{H}_{tw}$ also breaks the rotational symmetry of $\mathcal{H}_{tot}$ since Θ cannot be removed from $\mathcal{H}_{tot}$ via a unitary transformation. Thus the behavior of the energy gap in a transverse field will in general depend on Θ. It can be verified that, in the absence of external fields, the energy spectrum of $\mathcal{H}_{tot}$ is periodic in Θ with period $\pi/3$, which is a manifestation of the 60° rotation symmetry in the honeycomb lattice.

It is explicit in Eq. (69) that the effects of $\mathcal{H}_{tw}$ are the order of a_{cc}/R corrections to $\mathcal{H}_D$. Such effects are negligible for semiconducting NT's because of a large gap $\Delta_0/3$. In metallic NT's, however, the Hamiltonian $\mathcal{H}_{tw}$ plays an important role. In particular, the system described by the Hamiltonian (68) develops a minigap

$$\Delta_{tw} = \frac{2a_{cc}}{R}\Delta_0\,\frac{\phi^2|\cos 3\Theta|}{g_0(\phi)} \quad (71)$$

due to the magnetic field ϕ [defined in Eq. (16)]. This result can be obtained by projecting the perturbation $\mathcal{H}_{tw}$ taken at $k = 0$ onto the supersymmetric basis (39):

$$\mathcal{H}_{tw}|_{k=0} = -\frac{2a_{cc}}{R}\Delta_0\,\frac{\phi^2}{g_0(\phi)}\,\sigma_1 . \quad (72)$$

Note that the minigap (71) depends explicitly on the chiral angle Θ as $|\cos 3\Theta|$. Thus, for a given NT radius, Δ_{tw} reaches its maximum in zigzag NT's ($\Theta = 0$) and vanishes in armchair NT's ($\Theta = \pi/2$). The gap (71) is a manifestation of the broken supersymmetry. Minigaps of purely magnetic origin have been reported in Ref.[19] for zigzag and armchair NT's; however, the gap dependence on the chiral angle Θ was not discussed.

When the magnetic field is large, $\phi \sim 1$, the minigap Δ_{tw} is comparable to the curvature-induced minigap

$$\Delta_c = \frac{a_{cc}}{16R}\Delta_0|\cos 3\Theta|, \quad (73)$$

which is present in *zero* field.[2,3] In this situation, the two mechanisms for minigaps may compete and should be considered simultaneously. Instead of imposing the quasiperiodic boundary condition (19), we take the curvature effect into account in an alternative way[3] by introducing a pseudovector potential $\mathbf{A}^{(c)}$,

$$A_x^{(c)} + iA_y^{(c)} = i\frac{\Phi_0}{2\pi}\cdot\frac{a_{cc}}{16R^2}\,e^{3i\Theta} , \quad (74)$$

which should be added to the magnetic vector potential $\mathbf{A}(\mathbf{r})$. Surprisingly, the two gap opening mechanisms, Eqs. (69) and (74), interfere *destructively* at both the K and K' points and produce the gap

$$\Delta_\phi = \left|\frac{\Delta_c}{g_0(\phi)} - \Delta_{tw}\right| \quad (75)$$

in a moderate transverse magnetic field ($\phi \lesssim 1$). In particular, Δ_ϕ *vanishes* at $\phi = (4\sqrt{2})^{-1}$ due to the destructive interference.

VII. ELECTRON INTERACTIONS *VS.* SUSY

Electron interaction effects on NT's were addressed in various theoretical[25–29] and experimental[30] studies. Below we consider the effects of the repulsive interaction between electrons on the NT spectrum in the presence of a perpendicular magnetic field. As we have seen above in Secs. III and IV, supersymmetry of the single-particle problem makes nanotubes "more metallic" in a strong field by enhancing the density of states and suppressing the excitation gap at zero energy in metallic and semiconducting tubes correspondingly. It is also known that the repulsive interaction between NT electrons opens a small gap in an otherwise metallic tube[25] as well as enhances the excitation gap in a semimetallic tube,[26] making the tubes "less metallic." Below we study the competition between supersymmetry and repulsive electron interactions, and find that strong interactions drastically reduce the effect of supersymmetry. This happens because supersymmetry enhances electron interactions near half-filling as one would expect from the increase in the density of states (46).

In what follows we consider the case of a very strong magnetic field $\phi > 1$. The latter condition corresponds to an exponentially large effect of the field on the single-electron NT spectrum. For that reason we will neglect the Zeeman effect, which is linear in field.

We consider the interacting problem whose Hamiltonian in the forward scattering approximation[27] reads

$$\mathcal{H}_{\text{tot}} = \mathcal{H}_0 + \mathcal{H}_{\text{int}} \ , \tag{76}$$

where

$$\mathcal{H}_0 = \hbar v \int d\mathbf{r} \sum_{\alpha=1}^{4} \Psi_\alpha^\dagger \left\{ \left(i\partial_y - \frac{\delta}{R} \right) \sigma_1 - (i\partial_x + \varphi_y')\sigma_2 \right\} \Psi_\alpha \tag{77}$$

and

$$\mathcal{H}_{\text{int}} = \frac{1}{2} \sum_k \rho_{-\mathbf{k}} V(\mathbf{k}) \rho_{\mathbf{k}} \ . \tag{78}$$

Here the Hamiltonian (77) describes four noninteracting fermion flavors ($4 = 2_{\text{spin}} \times 2_{\text{valley}}$) in a nanotube with the bare gap $\Delta = \hbar v \delta/R$, subject to a perpendicular magnetic field, $\varphi(y) = 2\phi \sin(y/R)$, $\varphi_y' \equiv d\varphi/dy$, where the dimensionless field strength ϕ is defined in Eq. (16). The Dirac spinors Ψ_α are operators in the second-quantized representation. The Coulomb interaction between electrons is described by the Hamiltonian (78), where the total density in the forward scattering approximation reads

$$\rho(\mathbf{r}) = \sum_{\alpha=1}^{4} \Psi_\alpha^\dagger \Psi_\alpha \ , \tag{79}$$

with the $2K_0$ harmonics [K_0 defined in Eq. (3)] neglected. The electron-electron interaction potential in the presence of a substrate with a dielectric constant ε is

$$V(x,y) = \frac{2}{\varepsilon+1} V_0(x,y) \ , \tag{80}$$

where

$$V_0(x,y) = \frac{e^2}{\sqrt{h^2 + x^2}} \ , \quad h = 2R\sin(y/2R) \ . \tag{81}$$

The problem (76) is SU(4) invariant with respect to rotations in the space of the four fermion flavors Ψ_α.

Below we focus on the low-energy properties of the problem (76). This allows us to utilize the projection on the supersymmetric basis (39):

$$\Psi_\alpha(\mathbf{r}) = \chi_{1\,\alpha}(x)\psi_1^{(0)}(y) + \chi_{2\,\alpha}(x)\psi_2^{(0)}(y) \ , \tag{82}$$

where the factorization of motion along x and y holds due to the assumption that the magnetic field does not vary along the tube. Using Eq. (82) we will reduce the problem (76) to the one-dimensional one, bosonize it, and estimate the effect of interactions on the plasmon velocity and on the semimetallic gap.

Let us perform a projection of the problem (76) onto the basis (82). This can be done by integrating out the circumferential degree of freedom using the following separation of scales. The effects of magnetic field occur on the short scale of the tube radius R, for which the relevant energy scale is $\sim \hbar v/R$. The effect of the Coulomb interaction between electrons accumulates over a length scale that is much greater than R, as described below. Therefore the effective 1D description of the interacting NT electrons can be obtained by first integrating out the circumferential coordinate y in Eq. (76) and then taking into account the Coulomb effects. Thus we obtain the effective one-dimensional Hamiltonian

$$\mathcal{H}_{\text{eff}} = \hbar\bar{v} \int dx \sum_\alpha \chi_\alpha^\dagger \left(-i\partial_x \sigma_2 - \frac{\delta}{R}\sigma_1 \right) \chi_\alpha + \frac{1}{2} \sum_k \tilde{\rho}_{-k} \tilde{V}(k) \tilde{\rho}_k \ , \tag{83}$$

with the bare velocity reduced due to supersymmetry,

$$\bar{v} = \frac{v}{g_0(\phi)} \ , \tag{84}$$

similar to Eq. (44). Here g_0 is given by Eq. (51),

$$\chi_\alpha = \begin{pmatrix} \chi_{1\,\alpha} \\ \chi_{2\,\alpha} \end{pmatrix} \ , \tag{85}$$

the one-dimensional electron density (calculated from half-filling)

$$\tilde{\rho} = \sum_{\alpha=1}^{4} \chi_\alpha^\dagger \chi_\alpha \ , \tag{86}$$

and the 1D interaction potential at $kR \ll 1$

$$\tilde{V}(k) \simeq \frac{2e^2}{\varepsilon+1} \ln\left[1 + (kR)^{-2}\right] \ . \tag{87}$$

In writing Eq. (83) we dropped the terms of the order $[e^2/(\varepsilon+1)]\ln\phi$ that are small compared to $\tilde{V}(k)$ at $kR \ll 1$. These terms appear since at $\phi > 1$ the states $\chi_{1\,\alpha}$ and $\chi_{2\,\alpha}$ are localized on the opposite sides of the tube. Therefore strictly speaking the interaction between the same components of the spinor (85) is cut off on the scale of magnetic length (64) rather than of the NT radius.

With the difference between the short-distance cutoffs in the potential (87) neglected, the effective 1D Hamiltonian (83) remains SU(4) invariant. It can be bosonized in the standard way,[27] $\chi_\alpha \propto e^{i\Phi_\alpha}$. This procedure immediately yields the renormalized plasmon velocity for a metallic nanotube,

$$\tilde{v} = K^{1/2}(\phi)\frac{v}{g_0(\phi)} \ , \tag{88}$$

where the charge stiffness (or the dimensionless interaction strength)

$$K_q(\phi) = 1 + \frac{4g_0(\phi)}{\pi\hbar v}\tilde{V}(q) \tag{89}$$

is *enhanced* by the magnetic field. (By the tilde we denote the physical quantities in the presence of 1D interactions.) Thus the plasmon velocity suppression factor $\tilde{g}_0(\phi) \equiv [\tilde{v}(\phi)/\tilde{v}(0)]^{-1}$ due to the magnetic field is given by

$$\tilde{g}_0(\phi) = \left[\frac{K(0)}{K(\phi)}\right]^{1/2} g_0(\phi) \ . \tag{90}$$

It is *reduced* compared to the noninteracting value $g_0(\phi)$ because of the enhancement of the interaction strength due to the perpendicular magnetic field. For a large interaction strength $K \gg 1$, the effect of electron interactions on the supersymmetry is dramatic:

$$\tilde{g}_0(\phi) \simeq [g_0(\phi)]^{1/2} \propto e^{2\phi} \ , \tag{91}$$

effectively reducing the field strength $\phi > 1$ by a factor of 2 in the exponential.

Consider now the semimetallic gap in the presence of a magnetic field. In bosonized language, this gap is estimated as the energy of a composite soliton of the charge and flavor modes,[26,28] with its energy dominated by that of the charge mode at $K \gg 1$. The essential feature for the present analysis is that the effect of the magnetic field on the Gaussian part of $\mathcal{H}_{\text{eff}}$ *factorizes*, renormalizing the velocity $\bar{v}$, with the backscattering term $\delta/R \equiv \Delta(\phi)g_0(\phi)/\hbar v$ inside the integral in Eq. (83) *independent of the field*. A straightforward calculation shows that the perpendicular field reduces the *renormalized gap* by the factor (90) obtained for the plasmon velocity:

$$\tilde{\Delta}(\phi) = \frac{\tilde{\Delta}(0)}{\tilde{g}_0(\phi)} \ , \quad \tilde{\Delta}(0) \simeq K^{1/2}(0)D^{1/5}\Delta^{4/5}(0) \ . \tag{92}$$

Here $\tilde{\Delta}(0)$ is the (renormalized) semimetallic gap in the absence of the field and $D \simeq \hbar v/R$ is the one-dimensional bandwidth.

In Eq. (92) the value of K is assumed to be taken at $ql_{\text{ch}} \sim 1$, where $l_{\text{ch}} \gg R$ is the size of the charged soliton in the bosonized description.[26] The universal power law 4/5 in the gap renormalization (92) is valid in the limit $K \gg 1$. Equations (88) and (92) show that the characteristic supersymmetry features of the velocity and minigap

suppression persist in the presence of Coulomb interactions. However, the effect of the perpendicular magnetic field is strongly reduced by the electron interactions due to the density-of-states increase (46).

VIII. CONCLUSIONS

To conclude, we have shown that the interesting properties of the nanotube electron spectrum in a perpendicular magnetic field found in Ref.[7] can be understood as a consequence of supersymmetry of the low-energy NT Hamiltonian. We have demonstrated that supersymmetry ensures stability of the zero-energy state in metallic NT's and yields a corresponding enhancement of the density of states. In semiconducting NT's, supersymmetry leads to an energy gap suppression that can be observed in transport or tunneling measurements. We also considered the effects due to the trigonal warping interaction arising from higher-order gradient expansion terms that violate supersymmetry and lead to field-sensitive minigaps in the metallic NT spectrum. Finally, we have found that supersymmetry persists in the presence of electron interactions, but the reduction of both the renormalized plasmon velocity and the excitation gap is weakened due to effectively increased interaction strength.

[1] R. Saito, G. Dresselhaus and M. S. Dresselhaus, *Physical Properties of Carbon Nanotubes* (Imperial College Press, London, 1998).

[2] N. Hamada, S. Sawada, and A. Oshiyama, Phys. Rev. Lett. **68**, 1579 (1992); R. Saito *et al.*, Phys. Rev. B **46**, 1804 (1992).

[3] C. L. Kane and E. J. Mele, Phys. Rev. Lett. **78**, 1932 (1997).

[4] A. Kleiner and S. Eggert, Phys. Rev. B **63**, 073408 (2001).

[5] C. Zhou, J. Kong, and H. Dai, Phys. Rev. Lett. **84**, 5604 (2000).

[6] M. Ouyang, J. L. Huang, C. L. Cheung, and C. M. Lieber, Science **292**, 702 (2001).

[7] H. Ajiki and T. Ando, J. Phys. Soc. Jpn. **62**, 1255 (1993).

[8] J.-O. Lee *et al.*, Solid State Commun. **115**, 467 (2000).

[9] A. Rochefort, P. Avouris, F. Lesage, and D. R. Salahub, Phys. Rev. B **60**, 13824 (1999).

[10] M. S. C. Mazzoni and H. Chacham, Appl. Phys. Lett. **76**, 1561 (2000);
P. E. Lammert, P. H. Zhang, and V. H. Crespi, Phys. Rev. Lett.**84** 2453 (2000);
C. Kilic *et al.* Phys. Rev. B **62**, 16345 (2000).

[11] M. T. Figge, M. Mostovoy, and J. Knoester, Phys. Rev. Lett. **86**, 4572 (2001).

[12] X. Zhou, Hu Chen, and Ou-Yang Zhong-can, J. Phys.: Condens. Mattter **13**, L635 (2001); see also: cond-mat/0102094.

[13] D. S. Novikov, L. S. Levitov, cond-mat/0204499.

[14] For a review see F. Cooper, A. Khare, and U. Sukhatme, Phys. Rep. **251**, 267 (1995).

[15] G. S. Boebinger, A. H. Lacerda, H. J. Schneider-Muntau, and N. Sullivan, Physica B **294**, 512 (2001).

[16] J. Sims, A. Baca, G. Boebinger, H. Boenig, H. Coe, K. Kihara, M. Manzo, C. Mielke, J. Schillig, Y. Eyssa, B. Lesch, L. Li, and H. Schneider-Muntau, IEEE Trans. Appl. Supercond. **10**, 510 (2000).

[17] J. E. Muller, Phys. Rev. Lett. **68**, 385 (1992).

[18] R. Saito, G. Dresselhaus, and M. S. Dresselhaus, Phys. Rev. B **50**, 14698 (1994).

[19] H. Ajiki and T. Ando, J. Phys. Soc. Jpn. **65**, 505 (1996).

[20] D. P. DiVincenzo and E. J. Mele, Phys. Rev. B **29**, 1685 (1984).

[21] The intrinsic curvature shifts the Fermi momentum slightly and a minigap appears there rather than at the K point. Although the quasiperiodic boundary condition does not take into account the Fermi momentum shift, it still produces the gap and energy dispersion near the gap correctly.

[22] Y. A. Golfand and E. P. Likhtman, JETP Lett. **13**, 323 (1971).

[23] E. Witten, Nucl. Phys. B **188**, 513 (1981).

[24] In the present case zero modes exist for *spinless* Dirac electrons when the *total flux* through a NT surface is precisely zero. Zero modes for the case of a nonzero total flux for a spin-1/2 electron in 2D were found in B. A. Dubrovin and S. P. Novikov, Sov. Phys. JETP **52**, 511 (1980); Y. Aharonov and A. Casher, Phys. Rev. A **19**, 2461 (1979).

[25] Yu. A. Krotov, D.-H. Lee, and S. G. Louie, Phys. Rev. Lett. **78**, 4245 (1997); H. Yoshioka and A. A. Odintsov, *ibid.* **82**, 374 (1999).

[26] L. S. Levitov and A. M. Tsvelik, Phys. Rev. Lett. **90**, 016401 (2003); cond-mat/0205344.

[27] R. Egger and A. O. Gogolin, Phys. Rev. Lett. **79**, 5082 (1997); C. Kane, L. Balents, and M. P. A. Fisher, *ibid.* **79**, 5086 (1997).

[28] V. I. Talyanskii, D. S. Novikov, B. D. Simons, and L. S. Levitov, Phys. Rev. Lett. **87**, 276802 (2001); cond-mat/0105220.

[29] H.-W. Lee, H. C. Lee, H. Yi, and H.-Y. Choi, Phys. Rev. Lett. **90**, 247001 (2003).

[30] M. Bockrath, D. H. Cobden, J. Lu, A. G. Rinzler, R. E. Smalley, L. Balents, and P. L. McEuen, Nature (London) **397**, 598 (1999); Z. Yao, H. W. Ch. Postma, L. Balents, and C. Dekker, *ibid.* **402**, 273 (1999).